



## Surface Science Letters

## Electronic decoupling and templating of Co nanocluster arrays on the boron nitride nanomesh

Iván Brihuega<sup>a,\*</sup>, Christian Heinrich Michaelis<sup>a</sup>, Jian Zhang<sup>a</sup>, Sangita Bose<sup>a</sup>, Violetta Sessi<sup>a</sup>, Jan Honolka<sup>a</sup>, M. Alexander Schneider<sup>a,b</sup>, Axel Enders<sup>a,c</sup>, Klaus Kern<sup>a,d</sup>

<sup>a</sup>Max-Planck-Institut für Festkörperforschung, Heisenbergstrasse 1, D-70569 Stuttgart, Germany

<sup>b</sup>Lehrstuhl für Festkörperphysik, Universität Erlangen, Staudtstrasse 7, 91058 Erlangen, Germany

<sup>c</sup>Department of Physics and Astronomy, University of Nebraska, Lincoln, NE 68588-0111, United States

<sup>d</sup>Institut de Physique des Nanostructures, Ecole Polytechnique Fédérale de Lausanne, CH-1015 Lausanne, Switzerland

## ARTICLE INFO

## Article history:

Received 4 March 2008

Accepted for publication 29 April 2008

Available online 16 May 2008

## Keywords:

Scanning tunneling microscopy

Surface electronic phenomena

Insulating films

Nanostructures

Thin film structures

Boron nitride

Cobalt

## ABSTRACT

Positioning nanostructures and functional molecules at surfaces and engineering their local coupling behavior is a key challenge in nanotechnology. The recently discovered BN nanomesh on the Rh(111) surface is a potential candidate to combine both properties, templating on the nanometer-scale and electronic decoupling. By means of low temperature scanning tunneling microscopy and spectroscopy experiments we demonstrate this advantageous combination for the case of Co nanoclusters, which can be ordered in a hexagonal nanoarray with a nearest neighbor distance of 3.2 nm on the BN nanomesh. The detection of a Coulomb gap of  $\approx 160$  meV proves the electronic decoupling of the clusters from the rhodium substrate.

© 2008 Elsevier B.V. All rights reserved.

Templated growth, introduced nearly a decade ago [1,2] has provided a versatile route with respect to positioning and the fabrication of highly ordered arrays with ultimate density. Many of the nanotemplates are, however, metal or semiconductor surfaces [3], which introduce unwanted substrate coupling changing the properties of the individual nanostructures. The recent discovery of a single layer of hexagonal boron nitride (h-BN) providing a highly regular “mesh” with nanometric periodicity on the Rh(111) surface [4,5] has attracted much attention due to its promising potential applications. The BN nanomesh is a very stable system which survives temperatures above 1000 K and can be exposed to air [6] or liquid [5] without losing its unique properties. It has a 3.2 nm periodicity extending over very large regions, which opens the possibility of using it as a nanotemplate [4,5]. In addition, h-BN monolayers are known to be insulating [7,8] and therefore the BN nanomesh could be used as an ultrathin insulating template combining nanotemplating and electronic decoupling capabilities.

Ultrathin insulating systems offer the exceptional possibility of investigating the electronic properties of individual molecules and

nanostructures that are electronically decoupled from the substrate. These properties can be addressed locally by means of scanning tunneling spectroscopy (STS). STS has been an unrivaled technique to obtain the local electronic properties of metallic and semiconductor surfaces down to the atomic scale and very recently it has also been successfully used in the case of ultrathin insulating films on metal surfaces [9–20].

In this work, by covering a Rh(111) surface only partially by the BN nanomesh, we have been able to probe the electronic properties of the ultrathin BN monolayer and to compare it with the pristine metal surface. By means of STS we have detected a clear insulator character on the BN nanomesh, which presents an electronic gap of 5–6 eV in the density of states, in clear contrast with the metallic behavior detected on the Rh(111) surface. This electronic gap is present on the whole BN nanomesh region, which demonstrates that the BN nanomesh is indeed a continuous layer with no real pores. This is also consistent with our atomically resolved STM images. By means of buffer layer assisted growth (BLAG), we have deposited Co clusters on the partially covered surface. These Co clusters are laterally ordered on the BN nanomesh regions and randomly placed on the clean Rh(111) surface. Our STS spectra prove that only the Co clusters adsorbed on the BN nanomesh show Coulomb blockade effects whereas they show

\* Corresponding author. Tel.: +49 711 689 1638; fax: +49 711 689 1662.  
E-mail address: [i.brihuega@fkf.mpg.de](mailto:i.brihuega@fkf.mpg.de) (I. Brihuega).

metallic behavior on the Rh(111) surface. This clearly indicates that the presence of the BN nanomesh electronically decouples the Co clusters from the rhodium substrate.

The experiments were performed in an ultra-high-vacuum system equipped with a home-built low temperature STM. The sample preparation procedure was the following. First, we obtained clean Rh(111) surfaces from a Rh(111) single crystal by successive cycles of argon sputtering and annealing. Then, in order to prepare surfaces partially covered by the BN nanomesh, we exposed the clean surface to borazine gas while keeping it at 1070 K. Doses of 40 l ( $1 \text{ l} = 10^{-6} \text{ Torr s}$ ) of borazine already formed a complete BN layer. By decreasing this dose, we obtained partial coverages, and the fraction of surface covered by the BN nanomesh was approximately the dose used divided by 40 l. Even for doses as low as 5 l, regions covered by the BN nanomesh were always quite large. For the present experiments we used doses of 20 l, which gave rise to samples with half of the surface covered by the BN nanomesh. We used buffer layer assisted growth (BLAG) to deposit Co clusters. We first adsorbed a Xe buffer layer on the surface at 50 K, then deposited Co on top in order to minimize the interaction with the substrate and finally desorbed the Xe layer by warming up the sample to room temperature. After each stage of preparation we transferred the sample into the STM, where we carefully checked its cleanliness. All STM and STS data shown here were measured at a temperature of 4.2 K. STM data were acquired with a home-made software and analyzed using WSxM [21].

Typical STM images measured on the BN nanomesh show a regular hexagonal structure with a 3.2 nm periodicity (left part of Fig.

1a). On the BN nanomesh two different kinds of regions are detected: a brighter one which is continuously connected (“wires” on the following) and isolated darker regions with the appearance of cavities (named “pores”). This appearance can vary depending on the precise STM tip conformation, which has given origin to the existence of two different structural models for the BN nanomesh. Originally, a double layer model with real pores was proposed [4]. This double layer model is now challenged by a single layer one based on very recent density functional theory calculations [22] and STM experiments [5]. Our atomically resolved STM images are in perfect agreement with the one layer model. In these high resolution images (inset Fig. 1a), one can observe that the BN nanomesh is formed by a continuous layer and that the pore regions present a hexagonal arrangement of atoms with 2.5 Å periodicity coming from the BN layer (when imaging the Rh(111) surface with atomic resolution the periodicity obtained is 2.7 Å).

The general morphology of our partially covered samples is shown in Fig. 1a. We have the coexistence of regions covered by the BN nanomesh (left part of the image) together with clean Rh(111) regions (right). The interface between both regions is very clear and abrupt and sometimes takes place on the middle of a Rh(111) terrace (white arrow in the lower part of the image) while on other terraces the BN nanomesh growth is limited by a Rh(111) step edge (black arrow in the upper part of the image). We studied the apparent step height of the interface by means of bias voltage dependent STM images, as the ones shown in Fig. 1b–e, in order to obtain information on the conduction and valence band of the BN monolayers [17,18]. In Fig. 1f, both the apparent height of “pore”

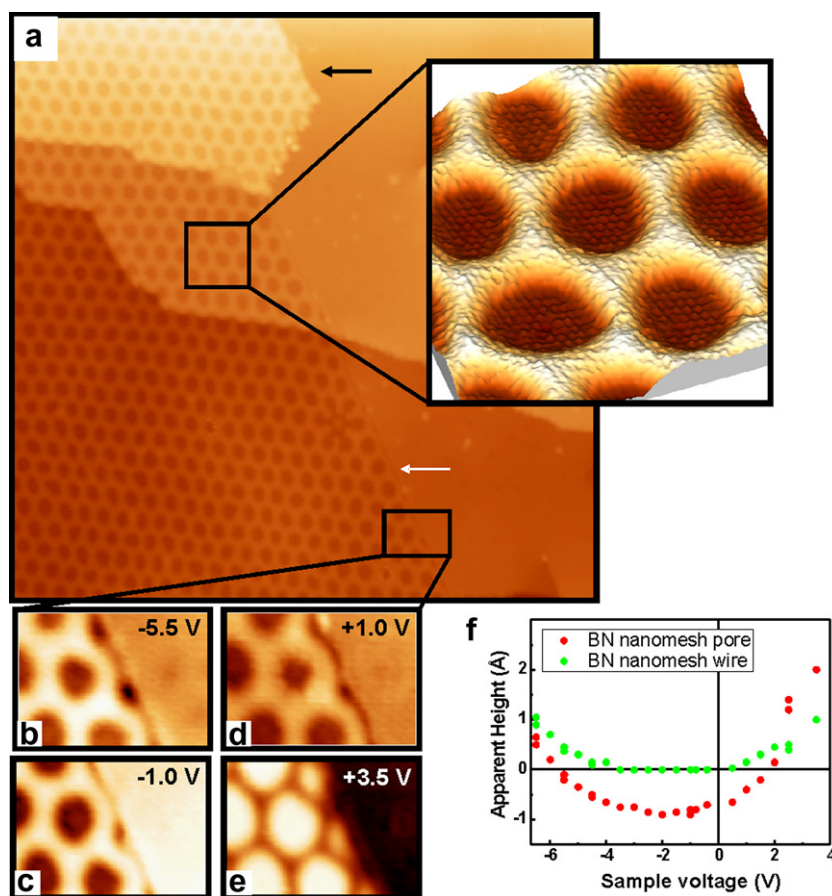


**Fig. 1.** (a) STM image showing the general morphology of the partially covered samples. Only the left part of the image the Rh(111) surface is covered by the BN nanomesh. The inset in (a) shows a  $10 \times 10 \text{ nm}^2$  BN nanomesh region with atomic resolution. (b)–(e) STM images of exactly the same interface region at different sample voltages. Depending on the voltage used the BN nanomesh appears higher or lower than the Rh(111) surface. (f) Graph with the voltage evolution of the apparent height of the BN nanomesh regions (wires and pores) compared to the Rh(111) clean surface. Image sizes  $100 \times 100 \text{ nm}^2$  (a),  $10 \times 7 \text{ nm}^2$  (b)–(e). Tunnel currents 0.2 nA (a), 1.0 nA (b)–(e). Sample voltages  $-1.0 \text{ V}$  (a),  $-5.5 \text{ V}$  (b),  $-1.0 \text{ V}$  (c),  $+1.0 \text{ V}$  (d), and  $+3.5 \text{ V}$  (e).

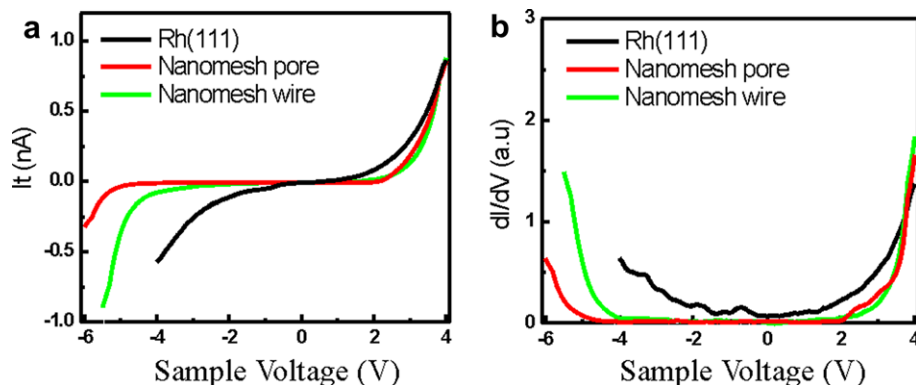


**Fig. 2.** (a)  $I$  vs  $V$  curves measured with exactly the same STM tip and tunneling conditions on the Rh(111) clean surface and on the BN nanomesh region. (b)  $dI/dV$  spectra extracted from (a) using a lock-in technique. The whole BN layer shows a clear insulating character presenting two different gap values of  $\approx 5$  eV for the “wire” regions (green curves) and  $\approx 6.5$  eV for the pore ones (red curves). (For interpretation of the references to colour in this figure legend, the reader is referred to the web version of this article.)

and “wire” regions measured with respect to the bare metal are plotted as a function of sample voltage. For relatively low biases the nanomesh appears with the same (“wires”) or lower (“pores”) height than the clean Rh(111) surface. Only when measuring at sufficiently high biases the nanomesh starts to appear higher than the Rh(111) surface. This indicates that when measuring at low bias the tunneling process is taking place through the BN nanomesh directly to the metal surface. This gives a first estimation of the band gaps with a value  $\approx 5$  eV for the “wire” regions and  $\approx 7$  eV for the “pore” ones.

Careful STS experiments were carried out at 4.2 K to extract the local electronic properties of the BN nanomesh. In order to obtain reliable STS data and to avoid tip artifacts, it is advantageous to have a reference for checking the STM tip configuration. In this work the clean Rh(111) surface, which coexists with the BN nanomesh, was used as such reference and only tips showing a clear featureless metallic character were taken into consideration in our STS analysis. We have mapped the whole surface by means of differential conductance ( $dI/dV$ ) spectra measured with open feedback loop using a lock-in technique. STS data were always acquired with initial tunneling parameters for which the BN nanomesh regions have a positive apparent height (see Fig. 1f). The reproducibility of all spectra was carefully checked by varying the initial tunneling current and hence the tip-sample distances and using different tips. Our experiments show that from the spectroscopic point of view both regions (“wires” and “pores”) show a marked insulating character, which definitely discards the possibility of the existence of real pores and clearly demonstrate that the BN nanomesh is a continuous insulating layer. Fig. 2 shows STS curves acquired on the BN nanomesh and on the Rh(111) surface with exactly the same STM tip and using identical tunneling parameters before opening the feedback loop. The experiments revealed a clear decrease of the conductance at low biases for the BN nanomesh regions compared to the Rh(111) surface. From the  $dI/dV$  spectra shown in Fig. 2b band gaps of  $\approx 5$  eV for the “wire” regions and of  $\approx 6.5$  eV for the “pore” regions are obtained. These values are very reproducible for all tunneling conditions and are in very good agreement with the ones initially inferred from the apparent height measurements discussed above.

Previous ultraviolet photoelectron spectroscopy data [4] showed the splitting of the BN band in two components at  $-4.6$  eV and  $-5.7$  eV, which were associated with two different layers of the BN nanomesh [4]. Very recently, it was suggested [5,22] that these peaks are associated with the “wire” and “pore” regions. Our STS spectra (see Fig. 2b) show that the BN  $\sigma$  peak positions correspond to the energies where an appreciable increase of the local density of states can be observed for “wires” (low energy

peak) and “pores” (high energy peak), confirming that they can be attributed to these regions.

In order to test the insulating capabilities of the BN nanomesh and to combine them with its templating effect, we deposited Co clusters using BLAG. In this way, the BN nanomesh acts as a template selectively accommodating Co clusters of almost identical size on the pores (see Fig. 3c). As shown in Fig. 3a, a highly ordered ensemble of Co clusters with a hexagonal 3.2 nm periodicity is obtained on the BN nanomesh regions, while a random distribution of Co clusters is found on the clean metal ones (see Fig. 3b). This demonstrates the templating capabilities of the BN nanomesh for metal clusters. The density of Co clusters on the BN nanomesh can be controlled by the number of BLAG cycles; filling factors up to 80% can be achieved [23]. When depositing Co on the partially covered surface, the clusters can be found on the Rh(111) clean surface as well as on the BN nanomesh regions as shown Fig. 4a. While Co clusters on the BN layer keep a nearly spherical shape, the clusters on the pristine Rh(111) surface flatten due to the large interfacial free energy.

By means of STS we studied the electronic properties of the Co clusters focusing on the role played by the BN nanomesh. Our results show the presence of an electronic gap in the Co clusters separated from the metal substrate by the BN layer. In small metallic clusters isolated from metallic electrodes, the tunneling process is affected by Coulomb blockade effects [24–27]. The addition of an electron into the cluster increases the energy of the system by a factor  $E_C = e^2/2C$ . If the capacitance  $C$  of the clusters is small enough, then this capacitive charging energy  $E_C$  is larger than the thermal energy  $k_B T$  and a Coulomb gap  $V_g = e/C$ , originating from the charging of the clusters by a single electron, is observed. For the present system, the capacitance of the Co clusters can be roughly estimated using a plate capacitor model  $C = \epsilon_0 \epsilon_{BN} A/d$ . Assuming for the BN layer a thickness  $d = 0.2$  nm [22,28] a dielectric constant  $\epsilon_{BN} = 4$  [29] and using the contact area  $A$  obtained from the STM topography, an approximate capacitance of  $C \approx 1 \times 10^{-18}$  F is estimated for a Co cluster of 2.7 nm diameter<sup>1</sup>. For this value of the capacitance a Coulomb gap  $V_g \approx 160$  meV is expected, which scales very nicely with the Coulomb gap width of the Co clusters adsorbed on the BN nanomesh (see Fig. 4b–c). Moreover, while all the spectra measured on Co clusters on the BN nanomesh show the Coulomb gap, STS spectra measured with exactly the same tip and stabilization conditions on Co clusters on

<sup>1</sup> The total Co Cluster capacitance is indeed formed by the addition of the Co cluster/substrate capacitance ( $C_{BN}$ ) and the STM tip/Co cluster capacitance ( $C_T$ ). However, for normal tunnel conditions  $C_{BN}$  should be much larger than  $C_T$ , thus, for the order of magnitude analysis used here we only take into consideration  $C_{BN}$ .

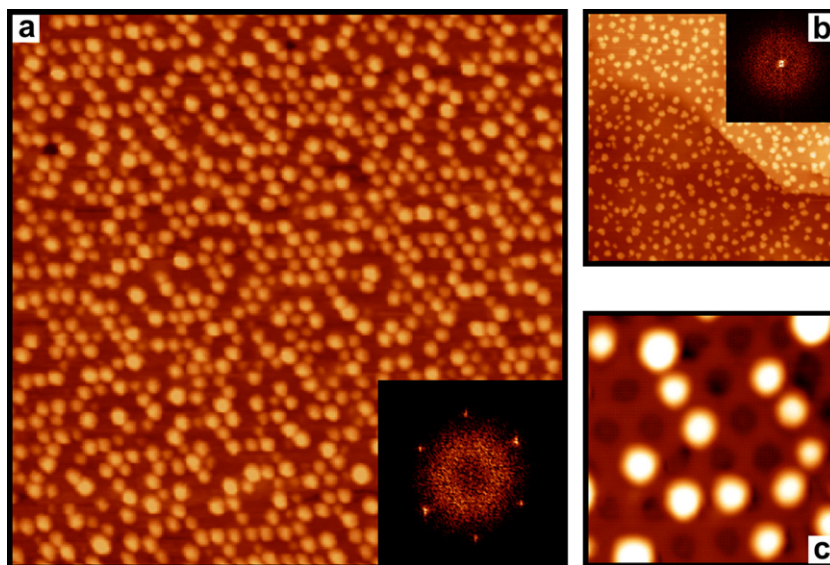


**Fig. 3.** (a) Large scale STM image demonstrating the lateral order of Co clusters deposited on top of the BN nanomesh using three cycles of BLAG. The inset shows its Fourier transform (FT). The six bright spots, originating from the Co cluster arrangement, match perfectly with the 3.2 nm hexagonal periodicity of the BN nanomesh. (b) Large scale STM image of Co clusters adsorbed on the clean Rh(111) surface. The absence of lateral order of these Co cluster is reflected in the fuzzy appearance with no bright spots of its FT shown in the inset. (c)  $17 \times 17 \text{ nm}^2$  STM image of the BN nanomesh after one Co deposition cycle where it can be observed how the Co clusters are placed on the pores of the BN nanomesh. Size of (a) and (b)  $100 \times 100 \text{ nm}^2$ . Tunnel currents and sample voltages are 1.2 V and 2.0 nA (a and b) 1.5 V and 0.1 nA (c).

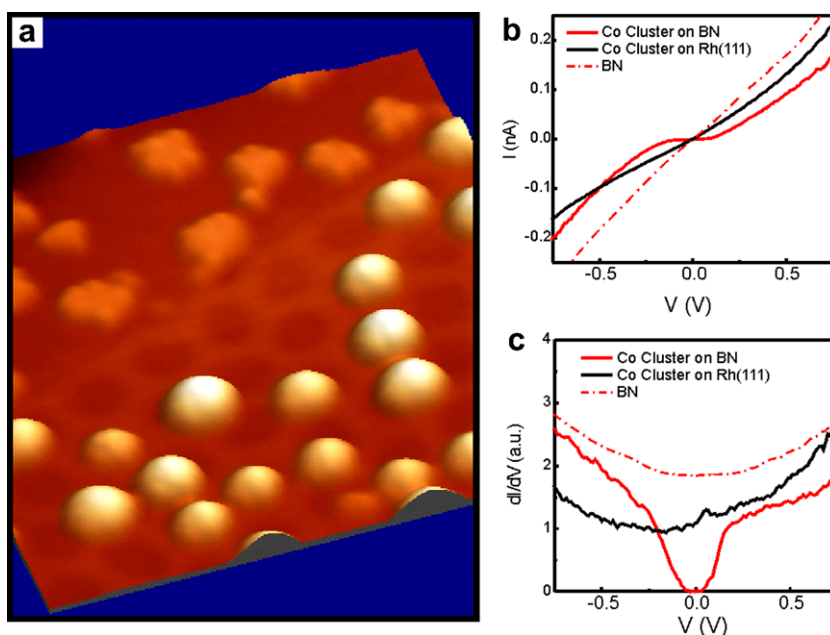


**Fig. 4.** (a)  $25 \times 25 \text{ nm}^2$  STM image of the partial covered surface after the Co deposition using BLAG. Co clusters can be observed both on the BN nanomesh region (bottom) and on the clean Rh(111) one (top). (b), (c)  $I-V$  (b) and  $dI/dV$  (c) spectra measured with exactly the same STM tip and stabilization conditions ( $I_t = 1.0 \text{ nA}$ ;  $V_{\text{sample}} = +1.5 \text{ V}$ ) on the bare BN nanomesh (red dashed curves), on top of a Co cluster adsorbed directly on the Rh(111) surface (black curves) and on top of a 2.7 nm diameter Co cluster adsorbed on the BN nanomesh (red curves). The BN nanomesh and the Co cluster in direct contact with the Rh(111) show a clear metallic behavior, while the Co cluster electronically isolated from the metal by the BN nanomesh presents an electronic gap due to Coulomb blockade effects (see text). (For interpretation of the references to colour in this figure legend, the reader is referred to the web version of this article.)

the Rh(111) surface show a clear metallic behavior (Fig. 4b–c). Reference spectra measured on the bare BN nanomesh with the same tip also show a metallic behavior (as explained above, when measuring on the BN nanomesh at these voltages electrons are directly tunneling into the metal) which excludes the possibility that the gap is also present on the BN confirming that it is an intrinsic feature of the Co cluster electronically isolated by the presence of the BN nanomesh.

In conclusion, by means of STS experiments we have proven that the BN nanomesh is a continuous layer with insulating and templating capabilities. The preparation of a partially covered surface allowed us to use the bare metal as a reference and also to investigate the influence of the BN layer on the electronic properties of deposited cobalt nanoclusters. Our results show that the combination of the insulating and templating properties of the BN nanomesh, together with the possibility of having at the same

time a clean metal surface, make the BN nanomesh an ideal playground for the study of the electronic properties of adsorbates electronically decoupled from the substrate.

### Acknowledgments

We thank Markus Weinmann for providing us the borazine. I.B. was supported by the European Community as part of a Marie Curie host fellowships for early stage researches training.

### References

- [1] H. Brune, M. Giovannini, K. Bromann, K. Kern, *Nature* 394 (1998) 451.
- [2] V. Holy, G. Springholz, M. Pinczolis, G. Bauer, *Phys. Rev. Lett.* 83 (1999) 356.
- [3] J.V. Barth, G. Costantini, K. Kern, *Nature* 437 (2005) 671.
- [4] M. Corso, W. Auwärter, M. Muntwiler, A. Tamai, T. Greber, *J. Osterwalder, Science* 303 (2004) 217.
- [5] O. Bunk, M. Corso, D. Martocchia, R. Herger, P.R. Willmott, B.D. Patterson, J. Osterwalder, I. van der Veen, T. Greber, *Surf. Sci.* 601 (2007) L7.
- [6] S. Berner, M. Corso, R. Widmer, O. Groening, R. Laskowski, P. Blaha, K. Schwarz, A. Goriachko, H. Over, S. Gsell, M. Schreck, H. Sachdev, T. Greber, *J. Osterwalder, Angew. Chem. Int. Ed.* 46 (2007) 5115.
- [7] A. Nagashima, N. Tejima, Y. Gamou, T. Kawai, C. Oshima, *Phys. Rev. Lett.* 75 (1995) 3918.
- [8] G.B. Grad, P. Blaha, K. Schwarz, W. Auwärter, T. Greber, *Phys. Rev. B* 68 (2003) 085404.
- [9] J. Repp, G. Meyer, F.E. Olsson, M. Persson, *Science* 305 (2004) 493.
- [10] X.H. Qiu, G.V. Nazin, W. Ho, *Phys. Rev. Lett.* 93 (2004) 196806.
- [11] A.J. Heinrich, J.A. Gupta, C.P. Lutz, D.M. Eigler, *Science* 306 (2004) 466.
- [12] J. Repp, G. Meyer, S.M. Stojkovic, A. Gourdon, C. Joachim, *Phys. Rev. Lett.* 94 (2005) 026803.
- [13] J. Repp, G. Meyer, *Appl. Phys. A – Mater. Sci. Process.* 85 (2006) 399.
- [14] S. Schintke, W.D. Schneider, *J. Phys. – Condens. Matter* 16 (2004) R49. and references therein.
- [15] W. Hebenstreit, J. Redinger, Z. Horozova, M. Schmid, R. Podloucky, P. Varga, *Surf. Sci.* 424 (1999) L321.
- [16] J. Viernow, D.Y. Petrovykh, A. Kirakosian, J.L. Lin, F.K. Men, M. Henzler, F.J. Himpsel, *Phys. Rev. B* 59 (1999) 10356.
- [17] A. Rosenhahn, J. Schneider, J. Kandler, C. Becker, K. Wandelt, *Surf. Sci.* 435 (1999) 705.
- [18] I. Sebastian, H. Neddermeyer, *Surf. Sci.* 454 (2000) 771.
- [19] S. Schintke, S. Messerli, M. Pivetta, F. Patthey, L. Libiouille, M. Stengel, A. De Vita, W.D. Schneider, *Phys. Rev. Lett.* 87 (2001) 276801.
- [20] G. Kresse, M. Schmid, E. Napetschnig, M. Shishkin, L. Kohler, P. Varga, *Science* 308 (2005) 1440.
- [21] I. Horcas, R. Fernandez, J.M. Gomez-Rodriguez, J. Colchero, J. Gomez-Herrero, A.M. Baro, *Rev. Sci. Instrum.* 78 (2007) 013705.
- [22] R. Laskowski, P. Blaha, T. Gallauner, K. Schwarz, *Phys. Rev. Lett.* 98 (2007) 106802.
- [23] J. Zhang et al., in preparation.
- [24] I. Giaever, H.R. Zeller, *Phys. Rev. Lett.* 20 (1968) 1504.
- [25] J. Lambe, R.C. Jaklevic, *Phys. Rev. Lett.* 22 (1969) 1371.
- [26] D.V. Averin, K.K. Likharev, *J. Low Temp. Phys.* 62 (1986) 345.
- [27] J.B. Barner, S.T. Ruggiero, *Phys. Rev. Lett.* 59 (1987) 807.
- [28] W. Auwärter, T.J. Kreutz, T. Greber, *J. Osterwalder, Surf. Sci.* 429 (1999) 229.
- [29] S.P.S. Arya, A. Damico, *Thin Solid Films* 157 (1988) 267.